Monte Carlo calculation of effective diffusivities in two- and three-dimensional heterogeneous materials of variable structure

Mark R. Riley,[1] Fernando J. Muzzio,[1,*] Helen M. Buettner,[1] and Sebastian C. Reyes[2]
[1]*Department of Chemical and Biochemical Engineering, Rutgers University, P.O. Box 909, Piscataway, New Jersey 08855-0909*
[2]*Corporate Research Laboratories, Exxon Research and Engineering Company, Route 22 East, Annandale, New Jersey 08801*
(Received 30 August 1993; revised manuscript received 17 December 1993)

A Monte Carlo technique that simulates tracer diffusion in multiphase materials of arbitrary complexity has been developed. Effective diffusivities are calculated for structures consisting of either overlapping or nonoverlapping inclusions with diffusivity D_c distributed in a continuous phase with diffusivity $D_0 > D_c$. Two-dimensional simulations for various values of D_0/D_c generate normalized diffusivities that correspond closely to their three-dimensional counterparts; they nearly collapse to a common curve when a simple scaling relation is applied.

PACS number(s): 51.10.+y, 66.30.Jt, 05.60.+w, 05.40.+j

Multiphase materials occur in a wide variety of systems, including polymer blends, ceramic precursors, soil, heterogeneous catalysts, and many types of biological tissue. These systems are often composed of one or more dispersed phases distributed in a single continuous phase. In general, the effective diffusivity of molecules through such materials depends on the volume fraction and solute mobility in each phase as well as on morphological details of the individual phases. Here, we present results of a Monte Carlo method that can be used to evaluate effective diffusivities of molecules in two-dimensional (2D) and three-dimensional (3D) multiphase materials with virtually any type of structure.

A substantial amount of experimental diffusivity data is available in the literature, but extrapolation of these measurements to other systems and conditions is generally difficult. Several approaches have previously been used by other researchers to predict diffusion in multiphase materials. Theoretical methods have led to a number of models, but the applicability of these models is frequently limited by restrictions on the geometric structure and volume fraction of the inclusions. For example, Maxwell's equation [1] assumes that the discrete phase occupies a small fraction of the total volume and consists of nonoverlapping, spherical inclusions randomly distributed in the continuous phase. In the context of diffusivities, Maxwell's equation can be written as

$$\frac{D_e}{D_0} = \frac{2D_0 + D_c - 2\phi(D_0 - D_c)}{2D_0 + D_c + \phi(D_0 - D_c)} , \tag{1}$$

where D_e is the macroscopic effective diffusivity, D_0 is the molecular diffusivity of the continuous phase, and D_c and ϕ are the molecular diffusivity and the volume fraction of the discrete phase, respectively.

Statistical approaches have been used to generate bounds for D_e (see, for example, [2]). However, the gap between bounds can be quite large, particularly when D_c differs significantly from D_0. A convenient approach is provided by Monte Carlo techniques, which have previously been used to study transport properties in a variety of macrostructures composed of inclusions that were either nonconductive [3] or more conductive than the continuous phase [4,5]. This paper focuses on a different case where the inclusions are permeable but their transport rates are lower than that of the continuous phase. Such a case has not been studied in detail before although it is relevant to many applications.

The first step in this Monte Carlo technique is to generate a computer representation of the macrostructure. The methodology is illustrated in this paper by generating two types of structure composed of either (i) overlappings inclusions or (ii) nonoverlapping inclusions distributed throughout a continuous phase. Circular inclusions are placed in a square region to simulate a 2D structure; spherical inclusions are placed in a cubic region to generate a 3D system. The placement region is spatially periodic, so that if an inclusion intersects the edge of the region, it partially reappears on the opposite side to account for the overhanging area. The structure with overlapping inclusions is produced by randomly positioning inclusions one at a time in the computational domain. If two (or more) inclusions overlap a given area, then this area is counted only once toward the total fractional coverage. To produce the nonoverlapping structure, inclusions are again placed one at a time until the desired inclusion fraction is attained. However, if the position of a new inclusion overlaps that of a previously placed inclusion, the new inclusion is rejected and another inclusion is placed in a different location. The process is repeated until the new inclusion is placed in an entirely open region. A small region of a representative 3D structure of nonoverlapping inclusions is depicted in Fig. 1. As noted by other researchers [4–6], this placement mechanism results in a nonequilibrium structure. However, as will be described shortly, the placement methodology has a relatively minor effect on the diffusive phenomena investigated here.

*To whom correspondence should be addressed.

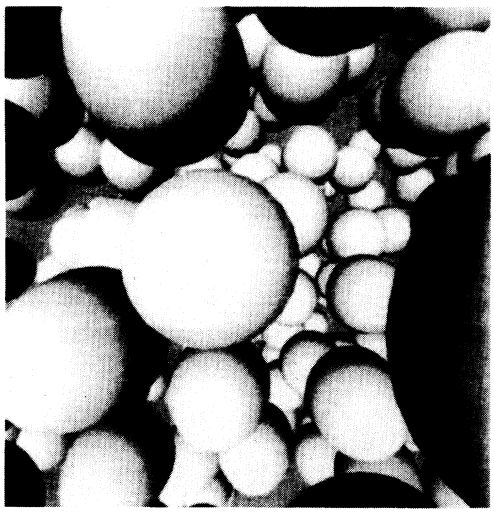

FIG. 1. Simulated 3D structure composed of nonoverlapping spheres randomly placed in a continuous domain. For this structure, the inclusion volume fraction is $\phi=0.30$.

To determine the diffusivity of molecules in these structures, tracer particles undergo a simulated random walk through the structural representation. Molecular diffusion in the continuous phase is described as a series of randomly directed steps with length $\lambda=\lambda_0 \ln\varepsilon$, where ε is a random number with uniform probability in the interval [0,1] and λ_0 is the mean step length in the continuous phase. Particles inside the inclusions take steps of length $\lambda=-\gamma\lambda_0\ln\varepsilon$, where $\gamma=D_c/D_0$ is a constant less than 1, reflecting the decrease in diffusivity inside the inclusions (D_c) relative to that in the continuous phase (D_0). The effective diffusivity is calculated by monitoring the distance traveled by the tracers in a certain amount of time. The straight-line displacement X between the initial and final positions of each tracer is used to calculate the mean-squared displacement $\langle X^2\rangle$ for a large number of tracers. For sufficiently many steps, the effective diffusivity is then calculated using the relationship

$$D_e=\frac{\langle X^2\rangle}{2d\sum\lambda}\ , \tag{2}$$

where d represents the dimensionality of the system and $\sum\lambda$, the total length of the walk, is proportional to the total time along the tracer's trajectory.

Because tracers in each phase are assigned different mean step lengths to account for different diffusivities in each phase, it is necessary to know at all times in which phase the tracer is located. To accomplish this, the simulation domain is discretized into a logical matrix array of one million nodes (1000×1000 for 2D simulations and $100\times100\times100$ for 3D simulations). The lattice is used only to discretize the spatial structure; the centers of the spheres are not regularly positioned on the lattice. Nodes within one inclusion radius from the center of an inclusion are assigned a logical value ·TRUE·, and all other nodes are assigned ·FALSE·. To determine the phase in which the tracer is located, the algorithm simply recalls the value of the node nearest the tracer; a returned value of ·TRUE· means the particle is inside an inclusion, while a value of ·FALSE· means the particle is in the continuous phase (a related approach was used by Kim and Torquato [5] to compute diffusivities in systems of partially overlapping highly conductive spheres). Although the structure chosen here for illustration is rather simple, the above discretization procedure is quite flexible and can be used to investigate essentially any type of structure because the procedure does not require inclusions with a regular geometry. Inclusions with variable morphology (spheroids, cylinders, irregularly shaped inclusions) or spatial arrangement (distinct, overlapping, or clustered inclusions) can also be readily described; clusters of coalesced spheres have been successfully simulated by this method [7]. Potentially, this technique could also be used to simulate diffusion through real structures by using digitized photographs of materials to generate the computational domain for simulations. This method has the additional advantage that 3D simulations require a similar amount of computer time as 2D simulations. This behavior is uncommon; as it is well known, computational time usually increases significantly with the dimensionality of the system.

Effective diffusivity results for freely overlapping circular inclusions in 2D are presented in Fig. 2(a). Results are displayed as normalized diffusivities (D_e/D_0) for inclusion fractions in the range $0\le\phi\le1$ and diffusivity ratios (D_0/D_c) ranging from 2 to 5. Results for uniformly distributed nonoverlapping inclusions in 2D and 3D systems are presented in Fig. 2(b) and 2(c), respectively, for inclusion fractions in the range $0\le\phi\le0.50$ (2D), and $0\le\phi\le0.45$ (3D) for diffusivity ratios from 2 to 5. These ranges of D_0/D_c and ϕ span experimental values reported for diffusivity measurements in systems of biological cells encapsulated in gelatinous supports [8]. Each point in Fig. 2 represents the average of ten structural realizations; each run was performed using the same number of inclusions placed in different positions. Each set of symbols corresponds to a given diffusivity ratio for varying inclusion fractions. Because $D_0/D_c>1$, effective diffusivities decrease with increasing inclusion fraction. The diffusivity also decreases as the inclusion diffusivity decreases; i.e., larger diffusivity ratios correspond to lower effective diffusivities D_e.

All the curves in Fig. 2(a) appear to have the same shape, except that they approach different lower limits as $\phi\to1$. This observation can be quantified by using a simple scaling relationship:

$$D^*(\phi)=\frac{[1-D_e(\phi)/D_0]}{(1-D_c/D_0)}\ . \tag{3}$$

This scaling removes the dependence on the diffusivity ratio by stretching the curves so that the bounds for $\phi=0$ and $\phi=1$ coincide for all sets of results [i.e., $D^*(0)=0$, $D^*(1)=1$ for all diffusivity ratios]. Rescaling the curves in Fig. 2(a) according to Eq. (3) makes the results nearly collapse onto a single curve [Fig. 3(a)]. For the overlapping inclusion structure, D^* is closely approximated for all sets of results by the following polynomial fit (solid curve in Fig. 3):

$$D^*=1.7271\phi-0.8177\phi^2+0.09075\phi^3\ . \tag{4}$$

This scaling technique also seems to work for nonoverlapping inclusions. As shown in Fig. 3(b), once the curves from Fig. 2(b) are rescaled according to Eq. (3), results corresponding to different diffusivity ratios again nearly collapse onto a single curve. Moreover, the same polynomial fit (4) as in Fig. 3(a) is used to represent rescaled diffusivities for nonoverlapping structures [Fig. 3(b)]. For the conditions investigated, the material structure does not affect D_e as the results for overlapping and nonoverlapping inclusions in 2D are nearly identical for a

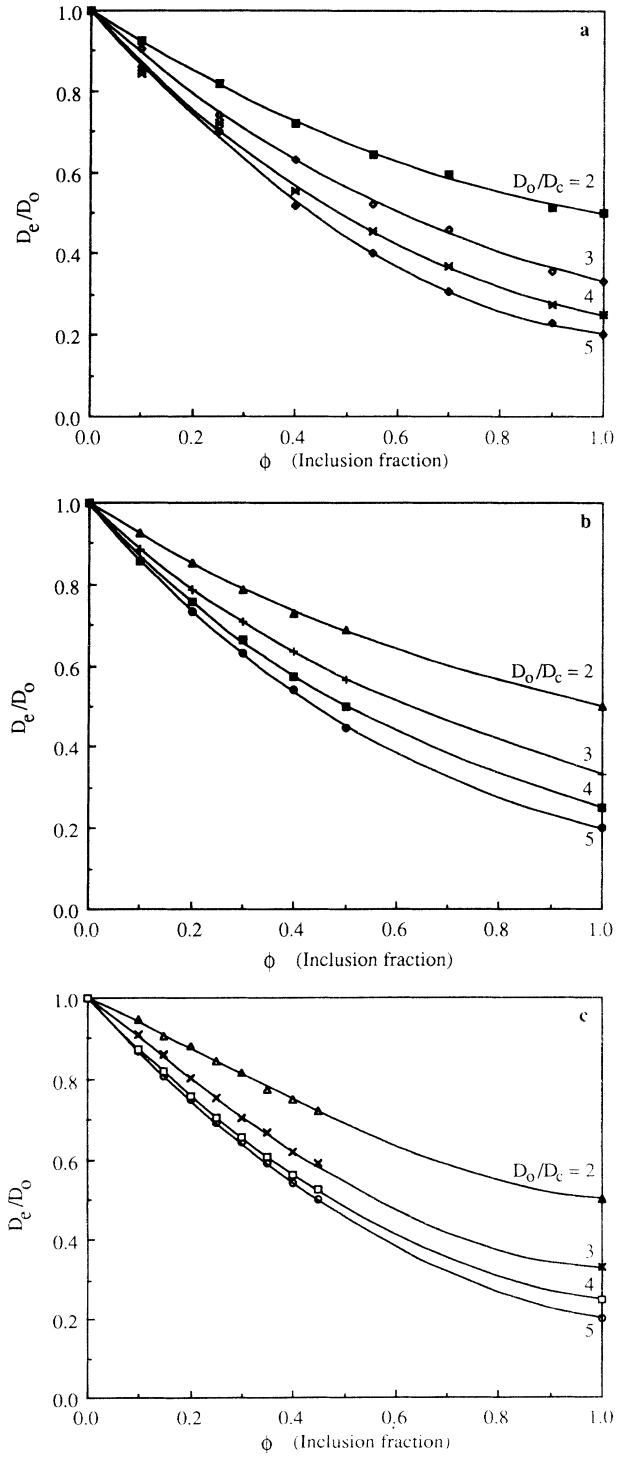

FIG. 2. Normalized effective diffusivities in 2D and 3D systems. Each point represents the average of ten simulation runs. Curves are polynomial least-squares fits to the results. (a) 2D diffusivities for overlapping inclusions; (b) 2D diffusivities for nonoverlapping inclusions; (c) 3D diffusivities for nonoverlapping inclusions.

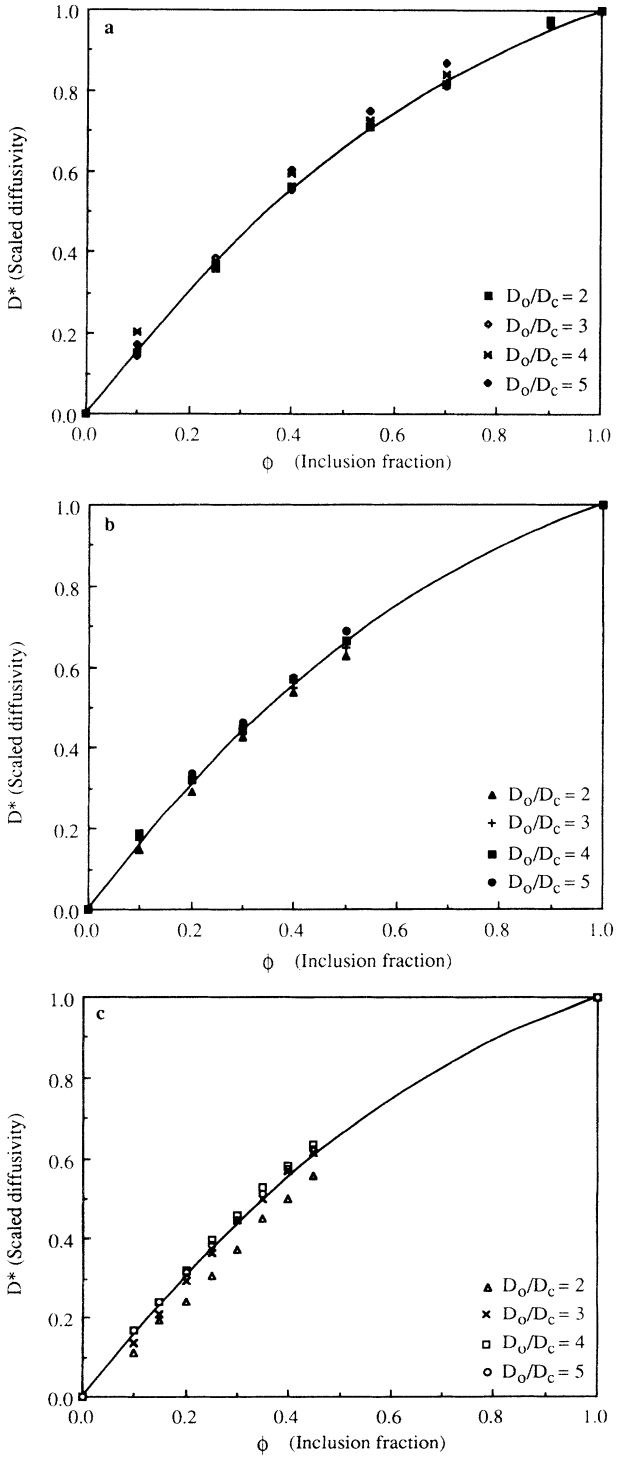

FIG. 3. Scaled diffusivities D^* of normalized diffusivities displayed in Fig. 2. The solid line corresponds to a third-order least-squares polynomial fit to the results. (a) 2D scaled diffusivities for overlapping inclusions; (b) 2D scaled diffusivities for nonoverlapping inclusions; (b) 3D scaled diffusivities for nonoverlapping inclusions.

given D_0/D_c and ϕ.

When the scaling Eq. (3) is applied to the 3D diffusivity predictions [Fig. 3(c)], results for $D_0/D_c=3,4,5$ again nearly collapse onto one curve. The poorest agreement is observed for $D_0/D_c=2$. For $D_0/D_c\rightarrow 1$, D^* approaches a straight line $D^*=\phi$ [this limit follows directly from Maxwell's model, Eq. (1)]. The case of $D_0/D_c=2$ can be regarded as a transition state between the straight-line limit and the fully developed curves for $D_0/D_c=3,4,5$ (and possibly beyond); rescaled results for $D_0/D_c=3,4,5$ are essentially identical to one another. Surprisingly, the 3D results are well represented again by *exactly the same polynomial fit* as the 2D results. Equation (4), therefore, closely predicts all the effective diffusivity values with less than 2–3% error for $D_0/D_c=3$, 4, or 5 for overlapping and nonoverlapping structures both in 2D and in 3D.

The similarity of the normalized diffusivities is further confirmed by comparing the unscaled simulation results in 2D and 3D both for overlapping and nonoverlapping inclusions (Fig. 4). For $D_0/D_c=3$ and 5, results from 2D and 3D simulations are almost identical. Results for $D_0/D_c=4$ (not shown for the sake of clarity of display) are also in excellent agreement with one another. Even for $D_0/D_c=2$, results from 2D and 3D simulations are quite similar both for overlapping and nonoverlapping cases. This agreement is entirely empirical and we do not presume that the correspondence is universal. This observation, however, has important practical implications, since it suggests that for some systems, 2D simulations can be used to predict diffusivities in 3D systems.

Finally, we note that Eqs. (3) and (4) can be combined to yield

$$D_e/D_0=1-(1-D_c/D_0)(1.7271\phi-0.8177\phi^2+0.09075\phi^3)\,. \quad (5)$$

This empirical relation can be used to predict effective diffusivities as a function of the inclusion fraction and the molecular diffusivities in the individual phases both for overlapping and nonoverlapping structures in 2D and for nonoverlapping structures in 3D. The predictions of Eq. (5) correspond to the three curves in Fig. 4. The simulation results have also been extensively compared with experimental data [7] and efficiently predict the trends in D_e as a function of ϕ and D_0/D_c.

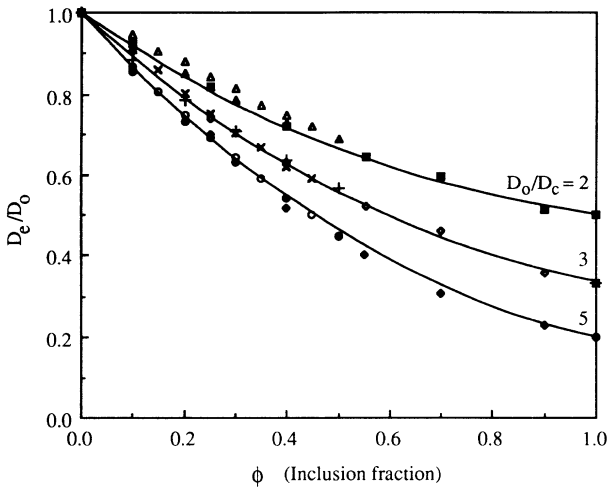

FIG. 4. Comparison of the effective diffusivity in 2D and 3D. Symbols are as in Figs. 2 and 3.

In summary, a Monte Carlo algorithm has been developed to calculate effective diffusivities of tracer particles in multiphase materials with virtually any type of structure. Results were illustrated for materials consisting of overlapping and nonoverlapping spheres randomly distributed in a continuous phase of higher diffusivity; other structures are considered elsewhere [7]. The predicted normalized diffusivities are largely independent of the dimensionality of the system; both for 2D and 3D simulations, diffusivities nearly collapse to the same curve when scaled using Eq. (3). An empirical relation developed for the prediction of diffusivities in 2D and 3D systems works reasonably well for all the cases considered here.

ACKNOWLEDGMENTS

This work was supported by grants from the Exxon Foundation and the Merck Foundation to F.J.M. and by a grant from the New Jersey Center for Biomaterials and Medical Devices to H.M.B. M.R.R. gratefully acknowledges Exxon Research and Engineering Company for financial support.

[1] J. C. Maxwell, *A Treatise on Electricity and Magnetism*, 3rd ed. (Dover, New York, 1954), Vol. 1.

[2] Z. Hashin and S. Shtrikman, J. Appl. Phys. **33**, 3125 (1962).

[3] J. W. Evans, M. H. Abbasi, and A. Sarin, J. Chem. Phys. **72**, 2967 (1980); K. A. Akanni and J. W. Evans, Chem. Eng. Sci. **42**, 1945 (1987); S. C. Reyes, E. Iglesia, and Y. C. Chiew, Mat. Res. Soc. Symp. Proc. **195**, 553 (1990); S. C. Reyes and E. Iglesia, J. Catal. **129**, 457 (1991).

[4] S. Y. Sheu, S. Kumar, and R. I. Cukier, Phys. Rev. B **42**, 1431 (1990).

[5] I. C. Kim and S. Torquato, J. Appl. Phys. **68**, 3892 (1990).

[6] N. Metropolis, A. W. Rosenbluth, M. N. Rosenbluth, A. N. Teller, and E. Teller, J. Chem. Phys. **21**, 1087 (1953).

[7] M. R. Riley, F. J. Muzzio, H. M. Buettner, and S. C. Reyes (unpublished).

[8] B. A. Westrin and A. Axelsson, Biotechnol. Bioeng. **38**, 439 (1991).

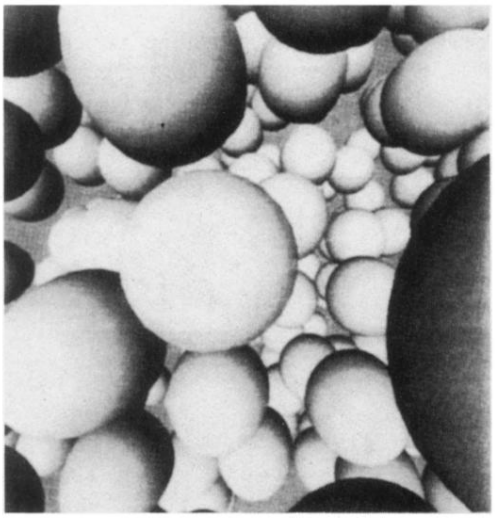

FIG. 1. Simulated 3D structure composed of nonoverlapping spheres randomly placed in a continuous domain. For this structure, the inclusion volume fraction is $\phi = 0.30$.